Experimental research on Textile Reinforced Concrete for the development of design tools

Patrick Valeri, Miguel Fernández Ruiz and Aurelio Muttoni

IBETON, Structural Concrete Laboratory,
École polytechnique fédérale de Lausanne,
Route Cantonale, Station 18, Lausanne (CH-1015), Switzerland

Abstract
Due to the limited construction experiences as well as to the absence of clear and consolidated design provisions for design of Textile Reinforced Concrete (TRC), the application of this material in practice is still very limited. In this paper, the results of an experimental programme are presented, with the aim of contributing to generate basic knowledge for development of consistent design tools. In particular, tensile tests on single textile strands and on the composite material have been performed. The experimental work is completed by structural tests on full-scale composite beams in simple bending. Finally, the experimental observations of the material behaviour and structural response are used to investigate on the pertinence of some simple mechanically-based models, reproducing TRC response based upon the key parameters of the material.

1 Introduction

At its early developments and in the last century, reinforced concrete was used to build thin-walled elements and lightweight structures, as shells or ferrocement laminar members. These applications have largely been abandoned during the last decades despite their high structural perfomance. This has been motivated both by durability (corrosion) issues and by construction needs. Current codes of practice recommend for instance minimal concrete covers between 25 and 55 mm to ensure durability. These cover requirements, as well as compacting needs, yield that RC structures are nowadays being associated to relatively heavy and massive works.

A possible approach to reduce the cover thickness to promote the use of light concrete structures has been identified by the use of non-corrosive reinforcement materials. In this sense, one of the most promising solutions is to embed textile reinforcement grids within a fine grained mortar. This is a relatively new composite material, commonly known as Textile Reinforced Concrete (TRC). The cementitious matrix is reinforced with several layers of a bidirectional, semi-flexible and high-performance fabric (carbon, basalt, glassfibers etc.). Currently, many different textile fabrics with varying properties are available on the market, giving large freedom to designers. With the potential to use various construction (pouring) techniques, very thin structural elements can be produced (generally with thicknesses lower than 20mm). Combined to the foldability of the reinforcement fabric, this composite becomes very attractive when it comes to double-curved structures or folded members.

Since the 1970's [1] and more intensively since the 1990's [2-6], several research centers have been investigating the new building material. Despite the previous research efforts, the state of knowledge of TRC is not yet sufficient to allow for a generalized use of it in structural engineering. Within this frame, the present research focuses on the material and structural behaviour of TRC by means of an experimental programme investigating the mechanical properties of a fine grained mortar and the fabric reinforcement as well as the structural behaviour in tension and simple bending. Finally, design approaches based on simple mechanical principles are outlined for the design of structural TRC-memebers.

2 Material behaviour

2.1 High performance cementitious mortar

For suitable casting of thin TRC elements, the concrete mix requires to have high flowability and a small aggregate size. For this research, a tailored mortar mix satisfying these requirements was used. The mortar was composed of nearly 40 % binder with low carbon blast furnace cement (CEM III/B) and a low amount of high quality micro silica and nearly 60 % aggregate (quartz powder and various

quartz sands). The low value of the mximum aggregate size (1.60 mm) ensures the penetration of the mortar in-between the reinforcement grid even for higher reinforcement ratios. A very low water-to-cement ratio was also used ($w/c \approx 0.25$) and combined with a superplasticizer to ensure high mechanical performance. The response of the mortar in compression was characterized on cylinders: $D = 70 \times H = 120$ mm. At 28 days, an average compressive strength (f_{cm}) of 110 MPa and a modulus of elasticity (E_{cm}) of 31.0 GPa were measured.

2.2 Textile Reinforcement

The textile reinforcement is composed by yarns (or filaments) grouped into rovings (bundles of yarns/strands) arranged in two directions to create a grid or fabric, see Fig. 1.

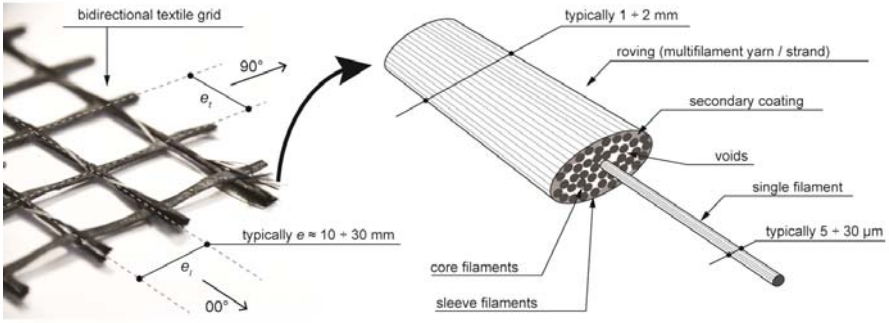

Fig. 1 Fabric Reinforcement: left, the textile strcure (and typical dimensions). Right, the structure of the multifilament yarn (and typical dimensions).

Yarns are made of the pure raw material (carbon, glass, basalt etc..) and have a very small diameter ($\emptyset_{fil} \approx 5 – 30$ µm), presenting thus high tensile strengths (for instance $f_{fil} \approx 5'000$ MPa for carbon fibres). Normally, a first primary coating is applied on the yarns (single filaments) in order to enhance their mechanical and durability properties.

With respect to the rovings, they are groups of hundreds or thousands of filaments, bundled together. Due to the large number of binding techniques of the yarns, it exists a wide spectrum of rovings with varying properties [7-8]. In addition, a secondary coating can also be applied at the surface of the roving or full impregnation of the filaments in order to enhance its properties (e.g., tensile strength, bond, etc…). The fineness of the rovings is typically measured in tex: 1tex = 1 g/km. Thus the active cross-section of a roving is calculated by means of the material density, as follows:

$$a_{Rov}\,[mm^2] = \frac{\text{linear density}}{\text{volumetric density}} = \frac{\lambda_{Rov}}{\rho_{mat}} \frac{\left[\text{tex} = \frac{\text{g}}{\text{km}}\right]}{\left[\frac{\text{kg}}{\text{m}^3}\right]}$$

As shown in Fig. 1, the cross-section of a roving is not completely filled by filaments and consequently the net cross-section is in general lower than the geometrical one. Rovings are eventually woven together to form the textile fabric, that is mostly bidirectional. The mechanical performance of textile reinforcement is thus usually characterized by its tensile strength in the two principal directions (longitudinal: dir.00° and transversal: dir.90°), provided per unit width of the fabric. Due to the fact that the tensile response is usually measured on single rovings, the unitary tensile strength is calculated as follows:

$$F_{u,grid}\,\left[\frac{\text{kN}}{\text{m}}\right] = \frac{\text{roving strength}}{\text{grid spacing}} = \frac{F_{u,Rov}}{e_{grid}} \frac{[\text{kN}]}{[\text{m}]}$$

Within this research project, 13 commercially available textile fabrics have been tested in their longitudinal and transversal directions. The seven more promising fabrics in terms of their mechanical properties are presented in Fig. 2, where it can be observed that carbon fibre fabrics (CF) have in general higher strength and stiffness than glass fibre fabrics (GF).

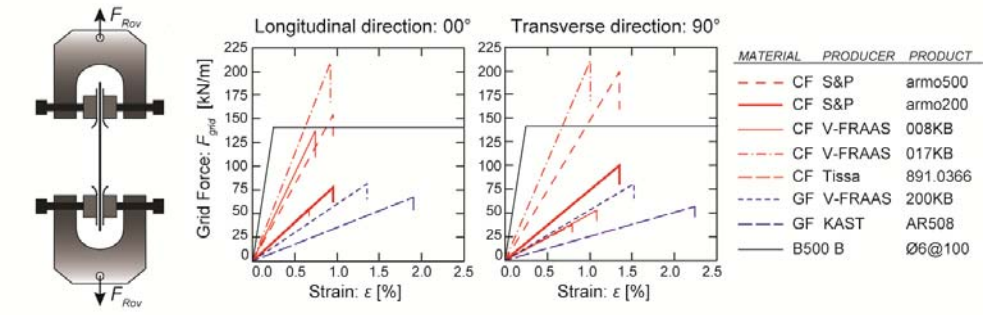

Fig. 2 Mechanical characterization of selected textiles: test set-up and tensile response in longitudinal (00°) and transversal (90°) directions.

Due to it's relatively better bond properties, resulting from an additional sand coating, the S&P ARMO-mesh® 200/200 has been selected for more detailed investigations. Further properties of this product are given in Table 1.

Table 1 Experimentally measured, mechanical properties of the S&P Armo-mesh® 200/200.

Property	Long. dir 00°	Transv. dir 90°	Unit
Linear density of strand: λ_{Rov}	2 × 800	1600	[tex]
Net roving cross-section: a_{Rov}	0.85	0.85	[mm^2]
Roving resistence: $F_{u,Rov}$	1450	1700	[N]
Roving strength: f_{Rov}	1700	2000	[MPa]
Roving modulus of elasticity: E_{Rov}	230	210	[GPa]
Grid spacing: e_{grid}	20	20	[mm]
Textile resistance: $F_{u,tex} = F_{u,Rov} / e_{grid}$	72.5	85	[kN/m]

2.3 Bond behaviour

In order to characterize the composite behaviour, several pull-out tets on sigle rovings have been performed (Fig. 3). These experiments are instrumental to understand the tensile behaviour of the investigated composite. In detail, single yarns have been embed in a short cylindrical segment. Within the experimental campaign, different embedment lengths were investigated, showing similar results (Fig. 3).

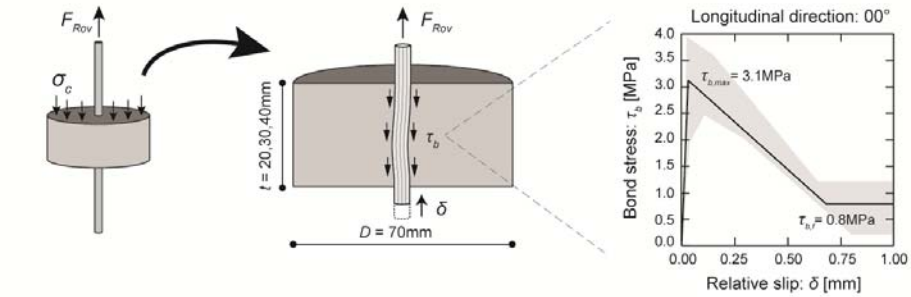

Fig. 3 Bond behaviour: test layout (left); specimen dimensions (center); experimental results for the longitudinal direction (right).

As shown in Fig. 3, the pull-out behaviour can be devided in three stages [9]: at first, the multifilament yarn exhibits a roughly linear response. After reaching the peak bond strength $\tau_{b,max}$, the bond exhibits a linear softening response until only a frictional bond component $\tau_{b,f}$ remains available. Furthermore, it was observed that SBR (Styrene Butadiene Rubber)-coated strands without additional sand-coating have significantly lower bond properties (for instance $\tau_{b,max} \approx 1.3$ MPa and $\tau_{b,f} \approx 0.3$ MPa), which can result in much longer anchorage lengths.

3 Tensile behavior of TRC

The tensile behaviour of TRC has been investigated on thin plates that can be considered representative of tensile zones in a structural member. To achieve a realistic reinforcement ratio, test specimens have been reinforced with several layers of the carbon textile fabric, aligned to the loading direction of the specimen (Figs. 4 and 5).

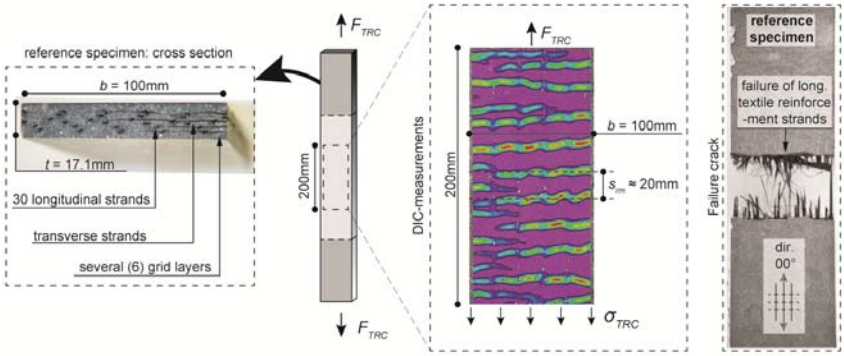

Fig. 4 Reinforcement layout (left); specimen (center); crack pattern and failure crack (right).

An instance of a tension specimen tested in this research is shown in Fig. 5, whose respose is characteristic for TRC-composites [10-13] and can be divided into three main different stages:

- **Stage I**: Uncracked response, when the stresses in the mortar are below its tensile strength;
- **Stage II**: Crack development stage, characterized by an increasing number of cracks developing for increasing load (or deformation);
- **Stage III**: Crack opening stage, characterized by a constant number of cracks in the element, whose widths increase for increasing load (or deformation).

Failure (Fig. 4), occurs within the Stage III in a sudden and brittle manner, and is mainly governed by the response of the reinforcement textile. As shown in Fig. 4, Detailed DIC (Digital Image Correlation) measurements reveal narrow crack spacing and low crack openings (up to 0.2 mm) at failure, showing good cracking performance for the investigated composite.

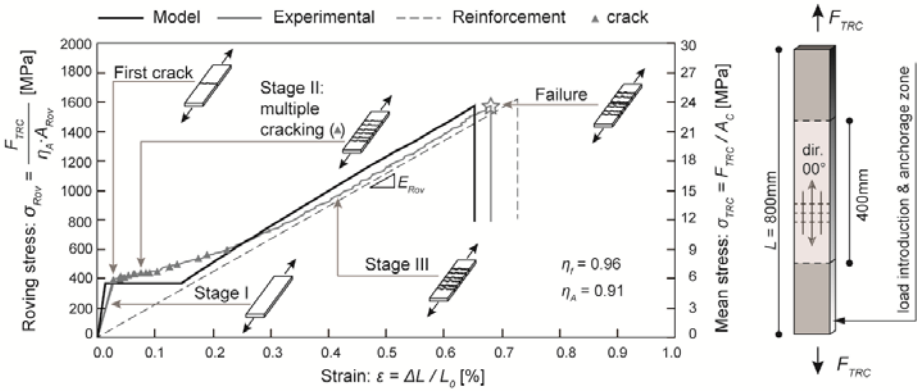

Fig. 5 Tensile response of Textile Reinforced Concrete reference specimen. Stress-strain curves, left, and specimen, right.

In Stage III, the response of the tie can be reproduced in a simple manner by considering the experimentally measured bond-slip law and by integrating the equilibrium (second order differential) equation govering bond:

$$\frac{d^2\delta}{dx^2} = \tau_b(\delta) \cdot \frac{U_{Rov}}{E_{Rov} \cdot \eta_A \cdot a_{Rov}}$$

Where U_{Rov} refers to the perimenter of a roving, E_{Rov} to its modulus of elasticity, a_{Rov} to the net roving cross section and η_A is an efficiency factor to account for the non-uniform distribution of stresses in the filaments of a roving. As shown in Fig. 5, the numerical integration of the elastic-cracked model gives satisfactory results.

With respect to the cracking (N_r) and failure (N_R) loads, they can be calculated as follows:

$$N_r = f_{ct} \cdot \left(A_{c,net} + \frac{E_{Rov}}{E_c} \cdot \eta_A \cdot A_{Rov}\right) \cong f_{ct} \cdot A_c$$

$$N_R = \eta_A \cdot \eta_f \cdot A_{Rov} \cdot f_{Rov}$$

Where η_f is the efficiency factor of the embedded fabric reinforcement (damage of crack lips on the filaments of a roving).

4 Flexural behaviour

The structural response in bending and shear has been investigated on TRC linear members. To that aim, an experimental programme consisting of two full-scale beams, tested on a 3–point-bending set-up has been carried out. Similar tests on smaller scale specimens have been previously carried out in other research centers [14-16]. The two test beams have been cast in the same formwork, resulting in the same geometry in terms of length and cross-section. As shown in Fig. 6, the first beam (BV1) has been reinforced with several layers of carbon textile fabrics and was designed to fail in bending. In order to avoid a flexural failure, the second beam (BV2) presents an additional metallic reinforcement in the bottom (tension) flange. This reinforcement was composed of seven, high strength, stainless-steel corrugated bars.

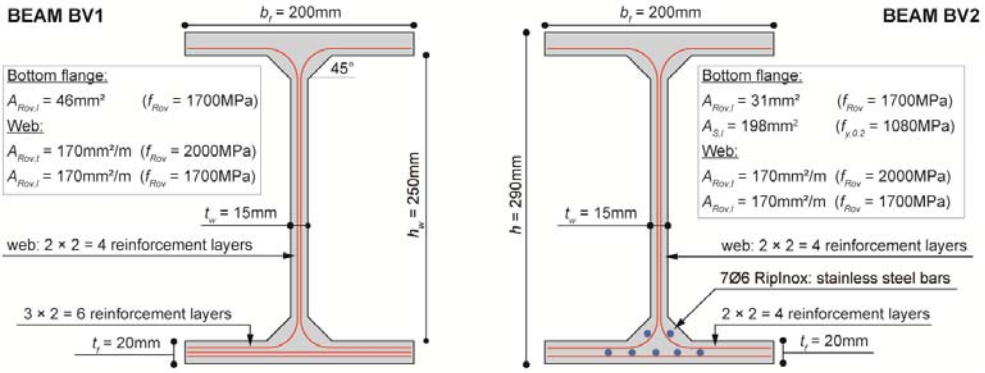

Fig. 6 Cross-section and reinforcement-layout of tested beams. Beam BV1, left: reinforced with fabric reinforcement only. Beam BV2, right: fabric and additional concentrated bottom reinforcement.

The flexural response of the tested beams, in terms of moment curvature at mid-span, is shown in Fig. 7. Beam BV1 failing in simple bending at mid-span at a moderate level and beam BV2 failing in shear (web-flange delamination) before attaining its maximum bending capacity. In fact, the higher bending resistance with respect to BV1, is to be attributed to the metallic reinforcement in the bottom flange, which presents a significantly larger cross-section than the textile ($A_{s,l} >> A_{Rov,l}$).

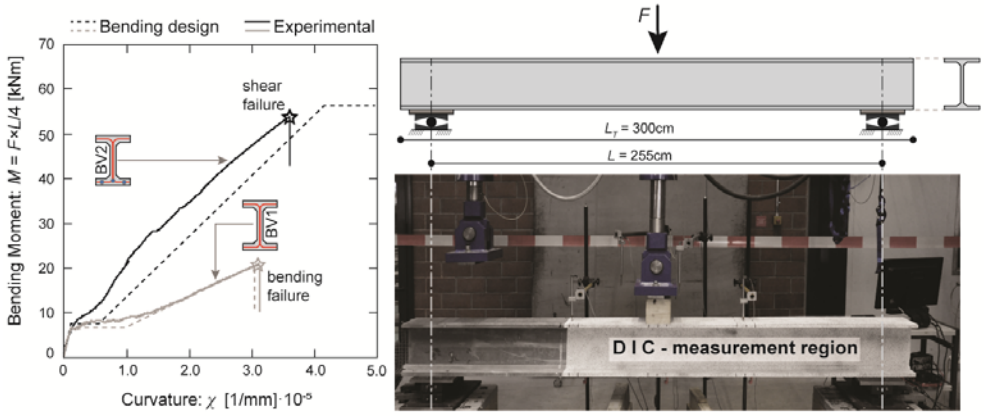

Fig. 7 Three-point-bending test set-up (right). Measured and calculated structural response in terms of moment curvature relation at mid-span (left).

Consistently with the behaviour in pure tension, a narrow crack pattern could be observed for both beams. As shown in Fig. 8 (pictures at 99% of the failure load), several closely-spaced bending cracks developed for beam BV1, whereas a typical shear crack pattern, with inclined cracks developed for beam BV2.

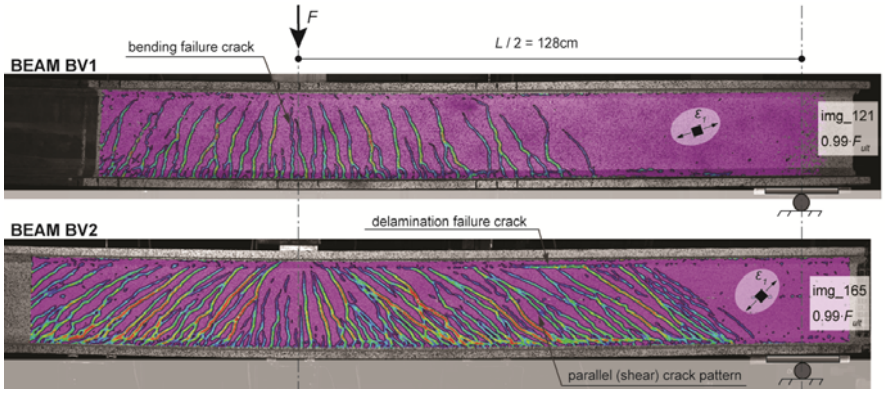

Fig. 8 Measured (DIC) crack patterns (principal tensile strains, ε_1) close to failure of the elements in the three-point-bending test. Beam BV1, top. Beam BV2, bottom.

In order to determine the resisting bending moment of linear members (M_R), the brittle nature of fabric reinforcement needs to be accounted for. In general, the fabric (and metallic) reinforcement might be distributed at different static depths. To account for the contribution of each layer (i) on the bending resistance, the stress in each layer (σ^i) is calculated by means of the Bernouilli's assumption (plane section remain plane) and computing their corresponding lever arm (z^i). Failure is reached when the fabric reaches its maximum strength ($\sigma_{Rov} = f_{Rov}$) or by steel yielding ($\sigma_s = f_{y,0.2}$):

$$M_{R,Rov} = \sum_{Rov} \left(\eta_A^i \cdot \eta_f^i \cdot \sigma_{Rov}^i \cdot A_{Rov}^i \cdot z_{Rov}^i \right)$$

In addition, due to its limited deformation capacity, the contribution of textile reinforcement can be neglected in presence of an additional ductile reinforcement.

$$M_{R,s} = \sum\nolimits_s \left(f_{y,0.2} \cdot A_s^j \cdot z_s^j \right)$$

Differently to bending, the shear behaviour in terms of failure load and kinematics is more difficult to reproduce. Numerical tools can thus become very helpful when it comes to understand a flexural

problem governed by shear. To that aim, it has been used in this research the Elasic-Plastic Stress Field approach (EPSF [17]), consistently used to investigate failures in shear in structural concrete members [18-19]. To apply this technique to TRC, the behaviour of the textile has to be considered as perfectly elastic until failure, whose limiting strain can be derived from the uniaxial tension response). This approach (Fig. 9) yields consistent results and is a promising approach for modelling of TRC cracked elements.

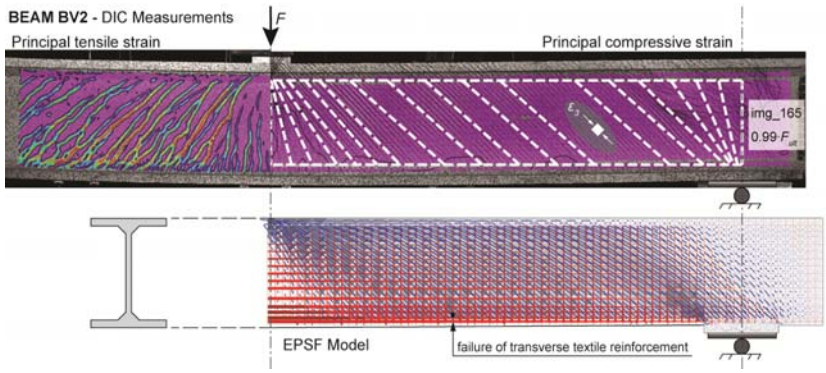

Fig. 9 Beam BV2: measured (DIC) crack patterns (principal tensile strains, ε_1), top-left; inclination of the compression field (principal strains ε_3), top-right. EPSF-model of the symmetric structure (compression field and reinforcement stresses), bottom.

5 Conclusions

This paper presents the results of an experimental programme designed to allow for development of consistent design tools for Textile Reinforced Concrete (TRC) as well as some potential modelling strategies for this material. Its main conclusions are:

- The bond conditions of the investigated TRC ensure low crack spacing and are associated to limited crack-opening for the tensile zones. Consistent modelling aproaches have been developed to characterize members in tension accounting for equilibrium and compatibility (bond-slip) conditions.
- With respect to bending on beams only reinforced with textile fabric, the strength is governed by the tensile strength of the TRC and failures happen in a brittle manner. A manner to enhance the strength and deformation capacity of beams consists of combining TRC with embed metallic (stainless steel) reinforcement. Consistent design methods can be used accounting for equilibrium and compatibility (Bernouilli's) conditions.
- Shear failures have a more complex nature, implying different potential phenomena, such as textile rupture, flange delamination and concrete crushing. The use of Elastic-Plastic Stress Fields (EPSF) as a general frame for modelling of TRC elements is a promising approach, accounting again for the equilibrium and compatibility conditions of the material.

Acknowledgements

The authors would like to sincerely acknowledge the support given by the association of the swiss cement producers: *cemsuisse* (research project #201407) for their financial support, providing the concrete mix and technical discussions.

References

[1] Aveston, J., and Kelly, A. 1973. "Theory of multiple fracture of fibrous composites" *Mater. Sci.* 8:352–362.

[2] Sadatoschi, O., and Hannat, D. J. 1994. "Modeling the Stress-Strain Response of Continuous Fiber Reinforced Cement Composites" *ACI Materials Journal* 91:306–312.

[3] Jesse, F. 2004. "Load Bearing Behaviour of Filament Yarns in cementitous matrix." PhD diss., Technische Univerität Dresden.

[4] Scholzen, A., Chudoba, R., and Hegger, J. 2015. “Thin-walled shell structures made of textile-reinforced concrete. Part I: Structural design and construction.” *Structural Concrete(2015)* 1:106–114.

[5] Scholzen, A., Chudoba, R., and Hegger, J. 2015. “Thin-walled shell structures made of textile-reinforced concrete. Part II: Experimental characterization, ultimate limit state assessment and numerical simulation.” *Structural Concrete(2015)* 1:115–124.

[6] Schumann, A., Michler, H., Schladitz, F. and Curbach, M. 2017. “Parking slabs made of carbon reinforced concrete.” *Structural Concrete(2017)*:1–9.

[7] Offermann, P., Engler, T., Gries, T. and Roye, A. 2004. “Technische Textilien zur Bewehrung von Betonbauteilen.” *Beton- und Stahlbetonbau* 99:437–443.

[8] Lorenz, L., Ortlepp, R., Hausding, J. and Cherif, C. 2011. “Effizienzsteigerung von Textilbeton durch Einsatz textiler Bewehrungen nach dem erweiterten Nähwirkverfahren.” *Beton- und Stahlbetonbau* 106:21–30.

[9] Aljewifi, H. 2012. “ Etude du comportement mécanique à l’arrachement de fils multi filametaires enrobés dans une matrice cimentaire et influence de l’imprégnation.” PhD diss., Université de Cergy-Pontoise.

[10] Bertolesi, E., Carozzi, F. G., Milani, G. and Poggi, C. 2014. “Numerical modeling of Fabric Reinforce Cementitious Matrix composites (FRCM) in tension.” *Construction and Building Materials* 70:531–548.

[11] RILEM Technical Committee (Brameshuber, W.), 2016. “Recommendation of RILEM TC 232-TDT: test methods and design of textile reinforced concrete. Uniaxial tensile test: test method to determine the load bearing behavior of tensile specimens made of textile reinforced concrete.” *Materials and Structures* 70:531–548. Accessed May 15, 2016. doi: 10.1617/s11527-016-0839-z.

[12] Larrinaga, P., Chastre, C., and Biscaia, H. 2014. “Experimental and numerical modeling of basalt textile reinforced mortar behavior under uniaxial tensile stress.” *Materials and design* 55:66–74.

[13] Contamine, R., Si Larbi, A., and Hamelin, P. 2011. “Contribution to direct tensile testing of textile reinforced concrete (TRC) composites.” *Materials Science and Engineering A* 528:8589–8598.

[14] Molter, M. 2005. “Zum Tragverhalten von textilbewehrtem Beton.” PhD diss., RWTH Aachen.

[15] Voss, S. 2008. “Ingenieurmodelle zum Tragverhalten von textilbewehrtem Beton.” PhD diss., RWTH Aachen.

[16] Kulas, C. 2013. “Zum Tragverhalten getränkter textiler Bewehrungselemente für Betonbauteile.” PhD diss., RWTH Aachen.

[17] Fernández Ruiz, M., Muttoni, A., 2007. “On development of suitable stress fields for structural concrete”, *American Concrete Institute, Structural Journal*, 104(4):495-502

[18] Rupf, M., Fernández Ruiz, M., Muttoni, A. 2013 “Post-tensioned girders with low amounts of shear reinforcement: shear strength and influence of flanges”, *Engineering Structures,* 56:357-371

[19] Muttoni, A., Fernández Ruiz, M., Niketic, F. 2015 “Design versus assessment of concrete structures using stress fields and strut-and-tie models”, *American Concrete Institute, Structural Journal*, 112(5):605-615